

Image Stego Detection using Higher Order Statistics

Assistant Lecturer Ammar Moufak J. Yousif
Department of Electrical Engineering,
Al-Mustansirya University
Email: ammar_farid2003@yahoo.com

Prof. Mahir K. AL-a'zawi
Department of Electrical Engineering,
Al-Mustansirya University

Abstract

The basic approach taken here works by finding predictable higher-order statistics of “natural” images within a multi-scale decomposition, and then showing that embedded messages alter these statistics. A Fisher linear discriminant analysis is then used to discriminate between untouched and adulterated images. Detection system suggested here is used to detect seven systems these are: hiding in LSB, hiding in palette, hiding in DCT simple level security, and hiding in wavelet simple level security. In addition, highly-secret systems were constructed, i.e. systems that integrate Cryptography with Steganography in both domains, DCT and Wavelet. Moreover, system of hiding in multiwavelet was used with cryptography.

Keywords: Steganography , Cryptography , Steganalytic .

1. Introduction

Steganography deals with hiding messages such that potential monitors don't even know that a message is being sent. It is different from cryptography where it is known that a secret message is being sent [1]. The term Steganography itself means “covered writing”.

Farid proposed a universal blind steganalytic detection method based on higher-order statistics of natural images [2]. Results for detecting steganographic messages being embedded with various publicly available steganographic programs (in both domain spatial and frequency) showed an astonishing performance of his method

Techniques for information hiding have become increasingly more sophisticated and widespread. With high-resolution digital images as carriers, detecting hidden messages has become considerably more difficult. This paper describes an approach to detect hidden messages in images. The approach uses a wavelet-like decomposition to build higher-order statistical models of natural images. A Fisher linear discriminant analysis (FLDA) [2] is then used to discriminate between untouched (original) and adulterated (stego) images. With digital images as carriers, detecting the presence of hidden messages poses significant challenges. Although the presence of embedded messages is often imperceptible to the human eye, it may nevertheless disturb the statistics of an image. Previous approaches to detect such

deviations [3,4,5,6] typically examine first-order statistical distributions of intensity or transform coefficients (e.g., discrete cosine transform, DCT). The drawback of this analysis is that simple counter-measures that match first-order statistics are likely foil detection. In contrast, the approach taken here relies on building higher-order statistical models for natural images [7,8,9] and looking for deviations from these models. Through a large number of natural images, it is proved that there exists strong higher-order statistical regularities within a wavelet-like decomposition. The embedding of a message significantly alters these statistics and thus becomes detectable.

2. The Detection Algorithm

The detection scheme can be separated in two parts. In the first part, a set of statistics is extracted, called the feature vector, for each investigated image. In the second part, a classification algorithm is used to separate original images from stego images by means of their feature vectors. Classification algorithm can be divided into classifier training and classifier testing for training images and testing images respectively.

In order to obtain the feature vector f of a certain image, a multi-level discrete two-dimensional (2-D) wavelet decomposition of that image is performed. Therefore, the image is decomposed in the approximation, vertical, horizontal, and diagonal subband by appropriate 2-D filtering and downsampling. The approximation subband is repeatedly decomposed in this way. The estimates for the first four (normalized) moments, namely the mean, variance, skewness, and kurtosis of the vertical, horizontal, and diagonal subbands for scales $i = 1, \dots, n-1$ form $4*3*(n-1)$ elements of f . Mean, variance, skewness, and kurtosis of a random variable x are defined respectively by :-

$\mu_x = E \{x\}$	1
$\sigma_x^2 = E \left\{ (x - \mu_x)^2 \right\}$	2
$\zeta_x = E \left\{ \left(\frac{x - \mu_x}{\sigma_x} \right)^3 \right\}$	3
$\kappa_x = E \left\{ \left(\frac{x - \mu_x}{\sigma_x} \right)^4 \right\}$	4

where $E \{ \cdot \}$ denotes the expectation operator. These moments are estimated using space

averaging and thus implying inherently stationarity and ergodicity of the subband coefficients. Obviously, this holds only to some degree for subband coefficients of natural images. The remaining elements of f are derived from the error statistics of an optimal linear predictor. Feature vector for each training images (cover and stego) is collected to create two matrices, one of them is called “stego” and the other is called “cover” (length of feature vector is the number of columns and number of images is the number of rows). These matrices are the input into classifier training. Moreover, two matrices will be created by collecting feature vectors for each testing images (cover and stego). The first matrix is called “stego” and the other is called “cover” (whereas feature vector length is the number of columns. The number of images will represent the number of rows). These matrices are the input into classifier testing. The whole detected process is illustrated in figure (1).

2.1 The Wavelet Decomposition

The decomposition of images using basis functions that are localized in spatial position, orientation and scale (e.g., wavelets) has been proven to be extremely useful in a range of applications (e.g., image compression, image coding, noise removal, and texture synthesis). One reason is that such decompositions exhibit statistical regularities that can be exploited (e.g., [10])

The initial aim here is to use the wavelet transform in the partitioning of the image into subbands in which each subband has certain information. The decomposition employed here is based on separable quadrature mirror filters (QMFs).

After extracting the coefficients of the wavelet, we will arrange them on the form of vector as illustrated in figure (2). This vector is named z . *Algorithm 1* is the summary of the wavelet decomposition stage.

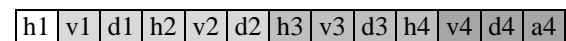


Figure (2) Vector (z) form of wavelet coefficients

Algorithm 1: Wavelet Decomposition
Input: Cover or Stego
Output: Wavelet coefficient, vector z
Step 1: Select the type of images (whether cover or stego).
Step 2: Input bases function (<i>Haar</i> function).
Step 3: Apply 4-level wavelet decomposition to image.
Step 4: Convert coefficient matrices into a vector as shown in figure (2).
Step 5: End

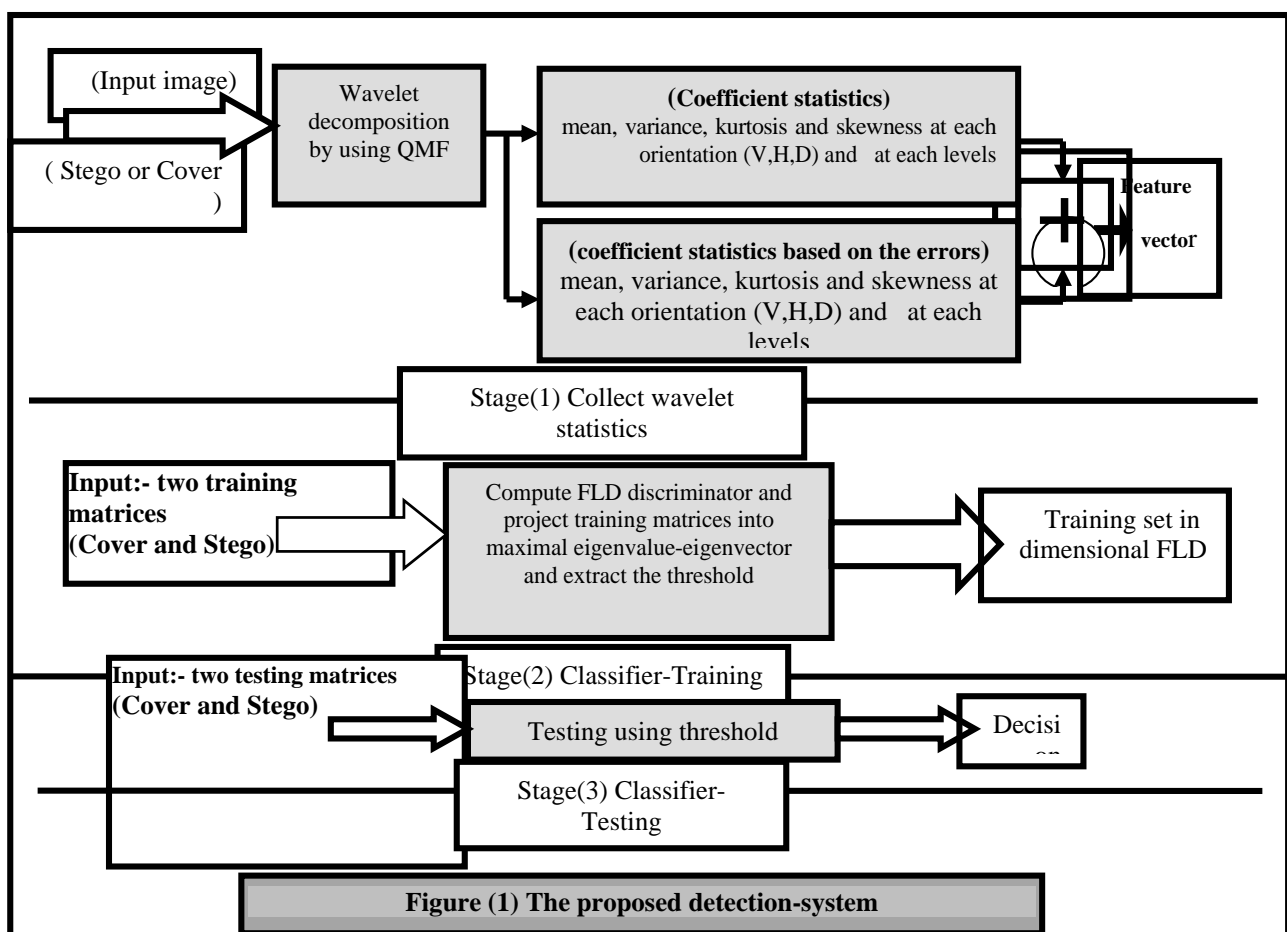


Figure (1) The proposed detection-system

2.2 Image statistics

Given this image decomposition, the statistical model is composed of the mean, variance, skewness and kurtosis of the subband coefficients at each orientation and at scales $i=1, \dots, n-1$. These statistics characterize the basic coefficient distributions. The second set of statistics is based on the errors in an optimal linear predictor of coefficient magnitude. As described in [10], the subband coefficients are correlated to their spatial, orientation and scale neighbors. For the purposes of illustration, consider first a vertical band, $V_i(x,y)$, at scale i . A linear predictor for the magnitude of these coefficients in a subset of all possible neighbors * is given by:

$$V_i(x,y) = w_1 V_i(x-1,y) + w_2 V_i(x+1,y) + w_3 V_i(x,y-1) + w_4 V_i(x,y+1) + w_5 V_{i+1}(x/2,y/2) + w_6 D_i(x,y) + w_7 D_{i+1}(x/2,y/2) \quad 5$$

where w_k denotes scalar weighting values*. This linear relationship is expressed more compactly in matrix form as:

$$\vec{V} = Q \vec{w} \quad 6$$

Where \vec{w} is the column vector $\vec{w} = (w_1, \dots, w_7)^T$. The vector \vec{V} contains the coefficient magnitudes of $V_i(x,y)$ strung out into a column vector, and the columns of the matrix Q contain the neighboring coefficient magnitudes as specified in Equation (5) strung out into column vectors. The coefficients are determined by minimizing the quadratic error function $E(\vec{w}) = [\vec{V} - Q\vec{w}]^2$. This error function is minimized analytically by differentiating with respect to \vec{w} :

$dE(\vec{w})/d\vec{w} = 2Q^T [\vec{V} - Q\vec{w}]$, setting the result to zero, and solving for \vec{w} , then:

$$\vec{w} = (Q^T Q)^{-1} Q^T \vec{V} \quad 7$$

The log error in the linear predictor is then given by:

$$\vec{E} = \log_2(\vec{V}) - \log_2(Q \vec{w}) \quad 8$$

From this error, the additional statistics are collected namely the mean, variance, skewness, and kurtosis. This process is repeated for each vertical subband at scale $i=1, \dots, n-1$, where at each scale a new linear predictor is

* The particular choice of spatial, orientation and scale neighbors was motivated by the observations of [10] and modified to include non-casual neighbors.

* $V_{i+1}(x/2, y/2)$ is used in order to avoid interpolation, the unsampled vertical subband (at position (x,y)) at scale $i+1$ is used. $H_{i+1}(x/2,y/2)$ and $D_{i+1}(x/2,y/2)$ are calculated the same way.

estimated. A similar process is repeated for the horizontal and diagonal subbands. The linear predictor for the horizontal subbands is of the form:

$$H_i(x,y) = w_1 H_i(x-1,y) + w_2 H_i(x+1,y) + w_3 H_i(x,y-1) + w_4 H_i(x,y+1) + w_5 H_{i+1}(x/2,y/2) + w_6 D_i(x,y) + w_7 D_{i+1}(x/2,y/2) \quad 9$$

And for the diagonal subbands:

$$D_i(x,y) = w_1 D_i(x-1,y) + w_2 D_i(x+1,y) + w_3 D_i(x,y-1) + w_4 D_i(x,y+1) + w_5 D_{i+1}(x/2,y/2) + w_6 H_i(x,y) + w_7 V_i(x,y) \quad 10$$

The same error metric, equation (8), and error statistics computed for the vertical subbands, are computed for the horizontal and diagonal bands, for a total of $12(n-1)$ error statistics. Combining these statistics with the $12(n-1)$ coefficient statistics yields a total of $24(n-1)$ statistics that form a feature vector which is used to discriminate between images that contain hidden messages and those that do not, where the input of the classification contains two matrices one matrix whose rows contain (no-stego) image feature vectors and the other matrix whose rows contain (stego) image feature vectors, where number of columns of matrices is the number of coefficient statistics 72 (if $n=4$) in the feature vector and the number of rows of matrices is the number of the images [2]. *Algorithm 2* is the summary of the above descriptions:-

Algorithm2:Collect statistics from sub-bands
Input: Vector z .
Output: Feature vector f .
Step1: Evaluating coefficients of vector z (mean, variance, kurtosis, and skewness) at each level and at each orientation by using equations (1), (2), (3), and (4).
Step2: Using linear predictor equation at each level and at each orientation to find predicted coefficients for vertical, horizontal, and diagonal by using equations (5), (9), and (10) respectively.
Step3: The result of the difference between the actual and predicted coefficients is the error as in equation (8) that is used to find (mean, variance, kurtosis, and skewness) at each level and at each orientation.
Step 4: Through collecting statistics found in actual coefficients as well as statistics found in error, feature vector f is found.
Step 5 : End

2.3 Classification

The 500 images chosen in this paper will be divided into training image and testing image where training image takes 400 images and testing takes 100 images. From the measured statistics of a training set of images with and without hidden messages, the goal is to determine whether a novel (test) image contains a message. To this end, Fisher Linear Discriminant analysis (FLD), a class specific method for pattern recognition, is employed. For simplicity a two –class FLD is described.

Denoted column vectors $\vec{x}_i, i = 1, \dots, N_x$ and $\vec{y}_j, j = 1, \dots, N_y$ as exemplars from each of two classes from the training set, and where $N_x=N_y= N$ is the number of images training, x refers to cover training images and y refers to stego training images. The within-class means are defined as:

$$\vec{\mu}_x = \frac{1}{N} \sum_{i=1}^N \vec{x}_i \text{ and } \vec{\mu}_y = \frac{1}{N} \sum_{j=1}^N \vec{y}_j \quad 11$$

The between-class mean is defined as:

$$\vec{\mu} = \frac{\vec{\mu}_x + \vec{\mu}_y}{2} \quad 12$$

The within-class scatter matrix is defined as [59]:

$$S_w = M_x M_x^T + M_y M_y^T \quad 13$$

Where, the i^{th} column of matrix M_x contains the zero-meaned i^{th} exemplar given by $\vec{x}_i - \vec{\mu}_x$. Similarly, the j^{th} column of matrix M_y contains $\vec{y}_j - \vec{\mu}_y$. The between-class scatter matrix is defined as:

$$S_b = N_x(\vec{\mu}_x - \vec{\mu})(\vec{\mu}_x - \vec{\mu})^T + N_y(\vec{\mu}_y - \vec{\mu})(\vec{\mu}_y - \vec{\mu})^T \quad 14$$

Finally, let \vec{e} be the eigenvector corresponding to maximal eigenvalue of S_b and S_w . When the training exemplars \vec{x}_i and \vec{y}_j are projected onto the one-dimensional linear subspace defined by \vec{e} , the within-class scatter is minimized and the between-class scatter is maximized.

$$proj_{trainingA} = \vec{x}_i^T \vec{e} \quad 15$$

$$proj_{trainingB} = \vec{y}_j^T \vec{e} \quad 16$$

For the purpose of pattern recognition, such a projection is clearly desirable as it simultaneously reduces the

dimensionality of the data and preserves discriminability. Once the FLD projection axis is determined from the training set, a novel exemplar, \vec{z} , from the testing set is classified by first projecting onto the same subspace :-

$$proj_{testingA} = \vec{z}_i^T \vec{e} \quad 17$$

$$proj_{testingB} = \vec{z}_j^T \vec{e} \quad 18$$

In the simplest case, the class to which this exemplar belongs is determined via a simple threshold. In the case of a two-class FLD, we are guaranteed to be able to project onto a one-dimensional subspace (i.e., there will be at most one non-zero eigenvalue). The training exemplar for stego and cover projected in FLD dimension will be converted into Receiver Operator Characteristic (ROC) plane, where in this plane the detection rate ranges from 50% (no detection rate) to 100% (full detection rate) therefore we will convert the detection rate ranging from (50-100)% represented by (y) to (0-100)% represented by (x) according to the equation:

$$x = 2y - 100 \quad 19$$

In ROC, intersection point among curves (stego and cover), the threshold value is created with false positive rate (i.e., a no-stego image incorrectly classified as a stego image). The threshold value will be used in testing exemplar into decision rate detection. A two-class FLD is employed here to classify images as either containing or not containing a hidden message. Each image is characterized by its feature vector as described in the previous section. *Algorithms 3 and 4* are the summary of the above descriptions:-

Algorithm3:Classifier- training

Input: Two matrices (stego and no-stego) whose columns are coefficients of feature vector. The rows represent the number of the training images.

Output: Stego and no-stego images are projected into two dimensional axes. The vertical axis corresponds to FLD whereas the horizontal axis corresponds to the number of the images (cover and stego). And finding threshold value.

Step1: Evaluate “within-class means” and “between-class means” by using equations (11) and (12) respectively.

Step2: Evaluate “within-class scatter matrix” (S_w) and “between-class scatter matrix” (S_b) by using equations (13) and (14) respectively.

Step 3: Find maximal real eign-value and eign-vector for two square matrix (S_b, S_w) in step 2 to create real vector (\vec{e}).

Step 4: Project training images (two matrices) on maximal eign-value and eign-vector (\vec{e}) (i.e., project on FLD axis) using equations (15) and (16).

Step 5: Find threshold value from ROC curve by the intersection between two curves (stego and cover).

Step 6 : End

Algorithm4:Classifier- testing

Input: Two matrices (stego and no-stego) whose columns are coefficients of feature vector. The rows represent the number of the testing images

Output: The decision

Step1: Project testing images (two matrices) on maximal eign-value and eign-vector (\vec{e}) (i.e., project on FLD axis) using equations (17) and (18).

Step2: Take threshold from classifier training for discrimination.

Step3: Decide detection rate with false positive rate with respect to threshold chosen for testing images.

Step 4: End

3. Results

Statistics from 500 such images are collected as follows. Each image is first converted from RGB to gray-scale using the well known equation (gray = 0.299R + 0.587G + 0.114B). A four-level, three-orientation QMF pyramid is constructed for each image, from which a 72-length feature vector of coefficient and error statistics is collected.

Messages are embedded into TIFF images (256x256) pixels using the following stego systems:-

1. **Hidden in LSB.**
2. **Hidden in palette.**
3. **Hidden in DCT simple level security.**
4. **Hidden in DCT high level security.**
5. **Hidden in wavelet simple level security.**
6. **Hidden in wavelet high level security.**
7. **Hidden in multiwavelet high level security.**

In these seven systems, images carrier, of fixed size (256 x 256) pixels and 256 gray scale, was used in an effort to conceal the secret image in sizes ranging from (16 x 16) pixels to (128 x 128) pixels and 256 gray scale. Algorithms software are

implemented with MATLAB 7.0 programming language with processor hyper- threading technology (2.8 G Hz), full cash.

In each case, a message consists of a $n \times n$ pixels ($128 \geq n \geq 16$) is used. The image fidelity criteria results for each method are illustrated in table (1) by taking maximum and minimum values of the tests (PSNR, and conditional entropy) from 500 images. The PSNR and conditional entropy are given by:

$$PSNR = 10 \log_{10} \frac{(L-1)^2}{\frac{1}{M * N} \sum_{r=1}^N \sum_{c=1}^M [I_2(r, c) - I_1(r, c)]^2} \quad 20$$

Where

N : height of the two images (because the two images must be of the same size).

M : width of the two images.

r and c : row and column numbers.

L : is the number of the gray scale level in the two images.

$I_1(r, c)$: is the original image.

$I_2(r, c)$: is the modified image.

$$H(I_1/I_2) = \sum_{i=1}^L P_{I_1}(i) \log_2 \frac{P_{I_1}(i)}{P_{I_2}(i)} \quad 21$$

Where

P_{I_1} :The probability distribution of the original image. P_{I_1}

P_{I_2} :The probability distribution of the modified image different from zero.

These probabilities are measured as

$$P_{I_1}(i) = \frac{n_{I_1}(i)}{n} \quad 22$$

$$P_{I_2}(i) = \frac{n_{I_2}(i)}{n} \quad 23$$

Here

$n_{I_1}(i)$:The number of pixels in the i^{th} gray level of the original image.

$n_{I_2}(i)$:The number of pixels in the i^{th} gray level of the modified image.

n : Total number of pixels in one image.

After the message is embedded into the cover image, the same transformation, decomposition, and collection of statistics as described above is performed.

The two-class FLD is trained on a random subset of 400 images and then tested on the remaining 100 images. Figure (3) shows the results for the training and testing set for hidden in palette system. In this figure the 'o' mark corresponds to "stego" images and the 'x' mark corresponds to the "no-stego" images. The

vertical axis corresponds to the value of an image feature vector after projecting onto the FLD projection axis. Results from the training set are shown to the left of the vertical line, and results from the testing set are shown to the right. The threshold for classification (horizontal line) is selected using the ROC curves shown in the lower part of figure (3).

In this part, the solid line corresponds to the percent of correctly classified no-stego images, and the dashed line corresponds to the percent of correctly classified stego images. The classification threshold is selected to be the point at which these curves cross.

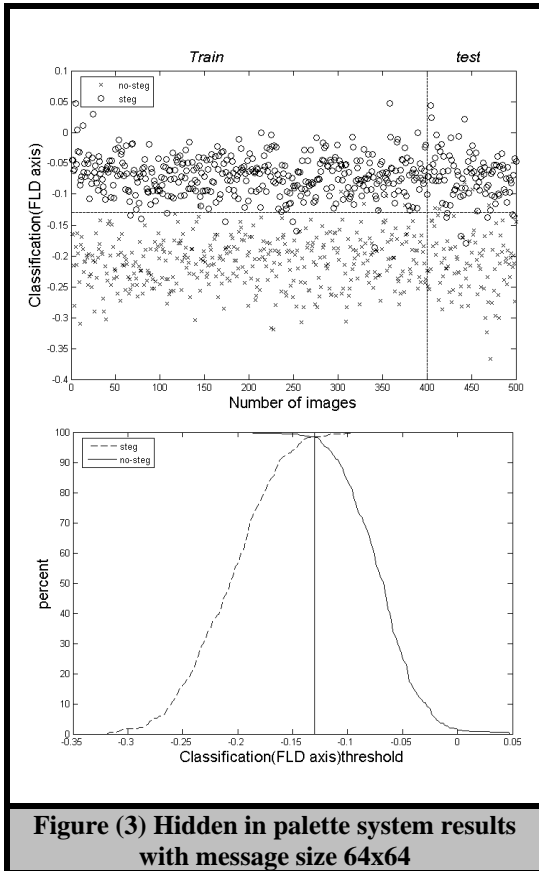


Figure (3) Hidden in palette system results with message size 64x64

Table (2) shows the results for one independent trial, where on this trial a random subset of 400 images are used for training, and the remaining 100 images are used for testing. The reported values, from the testing set, correspond to the accuracy of correctly classifying a stego image (detection rate), and of incorrectly classifying no-stego images (false positive rate corresponding into training images). This table shows the detection rate after using equation (19) and false positive rate, for message sizes ranging from 128x128 to 16x16 pixels. As the message size decreases, detection rates fall correspondingly. For the first method (Hidden in LSB), the message size ranges from 76x107 to 16x16 pixels. The detection rate decreases from 51.49% to 3.97% with false positive rate increase from 22.2% to 45.4% respectively.

Table (1) Image fidelity criteria results for seven different stego systems

Embedding	Message	PSNR (dB)		Conditional Entropy	
		Max.	Min.	Max.	Min.
Hidden in LSB	76 x 107	55.903	50.128	0.5826451775	0.0710516777
	64 x 64	56.478	52.984	0.3264474466	0.0505502820
	32 x 32	64.699	59.213	0.0842670577	0.0152594754
	16 x 16	70.648	65.233	0.0267745764	0.0059369534
Hidden in palette	64 x 64	48.962	32.368	0.0371858633	0.0124377246
	32 x 32	59.548	38.060	0.0191361379	0.0037734868
	16 x 16	66.146	43.785	0.0091581409	0.0009675245
Hidden in DCT with simple level security	76 x 107	308.254	85.156	0.0004843013	0.0000000000
	64 x 64	308.254	86.753	0.0003081491	0.0000000000
	32 x 32	308.254	90.275	0.0001761099	0.0000000000
	16 x 16	308.254	308.254	0.0000000000	0.0000000000
Hidden in DCT with high level security	128 x 128	54.556	51.006	0.5468044240	0.0791309172
	64x 64	61.118	56.659	0.1543143692	0.0234056254
	32 x 32	68.378	63.304	0.0384226128	0.0065099716
	16 x 16	80.275	68.979	0.0094249831	0.0012763883
Hidden in wavelet with simple level security	76 x 107	308.254	308.254	0.0000000000	0.0000000000
	64 x 64	308.254	308.254	0.0000000000	0.0000000000
	32 x 32	308.254	308.254	0.0000000000	0.0000000000
	16 x 16	308.254	308.254	0.0000000000	0.0000000000
Hidden in wavelet with high level security	128 x 128	53.860	51.874	0.3653087940	0.0615007431
	64 x 64	60.008	57.774	0.1074916999	0.0199130670
	32 x 32	66.695	64.168	0.0282253649	0.0059439879
	16 x 16	73.600	69.375	0.0097217816	0.0022011758
Hidden in multiwavelet with high level security	128 x 128	52.156	50.146	0.4788003280	0.0764680730
	64 x 64	58.432	56.005	0.1478213894	0.0249569136
	32 x 32	64.985	61.883	0.0450274677	0.0080573365
	16 x 16	72.230	67.869	0.0133958543	0.0030819205

For the second method (hidden in palette), the message size ranges from (64x64) to (16x16) pixels. The detection rate decreases from 87.13% to 13.87% with false positive rate from 1.63% to 43.4% respectively.

For the third method (hidden in DCT simple level security), the range of message sizes is the same as of LSB method. The detection rate decreases from 7.93% to 1% with false positive rate from 47.2% to 49.6% respectively.

For the fourth method (hidden in DCT with high level security), the message size range is the same as of LSB method. In this method, the detection rate decreases from 49.51% to 4.96% with false positive rate from 24.1% to 48.7% respectively.

For the fifth method (hidden in wavelet with simple level security) the message size range is the same as of LSB method. The detection rate decreases from 9.91% to 1% with false positive rate from 45.4% to 49.4% respectively.

For the sixth method (hidden in wavelet with high level security) the message size range is the same as of LSB method. The detection rate decreases from 45.55% to 1.99% with false positive rate from 20.9% to 44.3% respectively.

For the seventh method (hidden in multiwavelet with high level security) the message size range is the same as of LSB method. The detection rate decreases from 55.45% to 1% with false positive rate from 20.9% to 44.3% respectively.

Table (2) Classification accuracy for seven different stego systems

<i>Embedding</i>	<i>Message</i>	<i>Detection rate (%)</i>	<i>False positive rate (%) Corresponding into stego</i>
Hidden in LSB	76 x 107	51.49	22.2
	64 x 64	42.58	27.4
	32 x 32	18.82	39.7
	16 x 16	3.97	45.4
Hidden in palette	64 x 64	87.13	1.63
	32 x 32	36.64	27.4
	16 x 16	13.87	43.3
Hidden in DCT with simple level security	76 x 107	7.93	47.2
	64 x 64	4.96	42
	32 x 32	1.00	48.8
	16 x 16	1.00	49.6
Hidden in DCT with high level security	128 x 128	49.51	24.1
	64 x 64	26.74	37.8
	32 x 32	7.93	45.1
	16 x 16	4.96	48.7
Hidden in Pwavelet with simple level security	76 x 107	9.91	45.4
	64 x 64	2.98	47.3
	32 x 32	1.99	47.6
	16 x 16	1.00	49.4
Hidden in wavelet with high level security	128 x 128	45.55	24.2
	64 x 64	25.75	34.7
	32 x 32	6.94	43.6
	16 x 16	1.99	47.9
Hidden in multiwavelet with high level security	128 x 128	55.45	20.9
	64 x 64	30.7	31.2
	32 x 32	7.93	41.1
	16 x 16	1.00	44.3

4. Conclusions

The higher-order statistics appear to capture certain properties of "natural" images, and more importantly, these statistics are significantly altered when a message is embedded within an image. This makes it possible to detect, with a certain detection rate and false positive rate, the presence of hidden messages in digital images.

Although the system is tested on image messages, but it is also applicable for audio signals or video sequence, arbitrary image file formats, or other hiding algorithms.

The indiscriminant comparison of image statistics across all images could be replaced with a class based analysis, where, for example, indoor and outdoor scenes are compared separately.

From practical point of view, the size of the secret message in Steganographic system compared with cover size has a great effect on the detection rates.

The range of steganography systems security level has decreased to the level of cryptography. Thus, it became possible to know the presence of a secret message in steganography system.

In *PSNR* results ranging between 30 and 40 (db), we noticed that detection rate ranges between 80 and 90 (%). While in ranging between 50 and 55 (db), the detection rate ranges between 40 and 50 (%) and so on.

References

- [1]-D. Kahn, "*History of Steganography*", Information Hiding: First International workshop, Proceedings, Vol. 1174 of Lecture Notes in Computer Science, Springer, PP 1-5, 1996.
- [2]-Hany Farid, "*Detecting Hidden Messages Using Higher-Order Statistical Models*", Depart. Of Computer Science, Dartmouth College, Hanover NH 03755, 2002.
- [3]-N. F. Johnson and S. Jajodia, "*Steganalysis of Images Created Using Current Steganography Software*", Information Hiding: Second International Workshop, Proceedings, Vol. 1525 of Lecture Notes in Computer Science, Springer, PP 273-289, 1998.
- [4]-Provos, N. and Honeyman, P. "*Detecting Steganographic Content on the Internet*", Center for Information Technical Integration, University of Michigan, CITI Technical Report 01-11, 2001.
- [5]-Fridrich, J. and Goljan, M. "*Practical Steganalysis-State of the Art*" In Proc. of SPIE Security and Watermarking of Multimedia Contents IV, San Jose, California, Jan 2002.
- [6]-A. Westfeld and A. Pflizmann, "*Attacks on Steganographic Systems*", In Proceedings of Information Hiding, 3rd International Workshop, Dresden, Germany, 1999.
- [7]-D. Kersten, "*Predictability and Redundancy of Natural Images*", Journal of the Optical Society of America A, 4(12): 2395-2400, 1987.
- [8]-D. L. Ruderman and W. Bialek, "*Statistics of Natural Image*", Scaling in the Woods. Phys. Rev. Letter, 73(6): 814-817, 1994.
- [9]-E. P. Simoncelli, "*Modeling the Joint Statistics of Images in the Wavelet Domain*", In Proceedings of the 44th Annual Meeting, Volume 3813, Denver, CO, USA, 1999.
- [10]-R.W. Buccigrossi and E. P. Simoncelli, "*Image Compression Via Joint Statistical Characterization in the Wavelet Domain*", IEEE Transactions on Image Processing, 8(12): 1688-1701, 1999.

كشف الصورة المخفية باستخدام الإحصاءات ذات المرتبة العالية

ماهر خضير العزاوي
استاذ

قسم الهندسة الكهربائيه / الجامعة المستنصرية

عمار موفق يعقوب يوسف
مدرس مساعد

قسم الهندسة الكهربائيه / الجامعة المستنصرية

الخلاصة

إن الأسلوب الرئيسي المتبع هنا يعمل عبر إيجاد إحصائيات ذات تنظيم عال قابل للتنبؤ للصورة الطبيعية خلال تحليل متعدد المستويات ومن ثم عرض تغيير الرسائل المطمورة لهذه الإحصائيات. ويستخدم من بعد ذلك تحليل فيشر التحليلي الخطي في التمييز بين الصورة الأصلية و المطمورة. أستخدم نظام الكشف المقترح في كشف سبع أنظمة وهي: الإخفاء في LSB ، الإخفاء في Palette ، الإخفاء في DCT مع مستوى سرية بسيط ، والإخفاء في Wavelet مع مستوى سرية بسيط. وبالإضافة إلى ذلك ، تم بناء أنظمة عالية السرية وبمعنى آخر الأنظمة التي تدمج الكتابة السرية والكتابة المغطاة في المجالي DCT و Wavelet والأكثر من ذلك أستخدم الإخفاء في Multiwavelet مع الكتابة السرية.

This document was created with Win2PDF available at <http://www.daneprairie.com>.
The unregistered version of Win2PDF is for evaluation or non-commercial use only.